

**VIBRATION ANALYSIS OF A GIROMILL-TYPE
VERTICAL AXIS WIND TURBINE**

**A Thesis Submitted to
the Graduate School of Engineering and Sciences of
İzmir Institute of Technology
in Partial Fulfillment of the Requirements for the Degree of**

MASTER OF SCIENCE

in Mechanical Engineering

**by
Melih AKGÜNEYLİ**

**December 2013
İZMİR**

We approve the thesis of **Melih AKGÜNEYLİ**

Examining Committee Members:

Prof. Dr. Bülent YARDIMOĞLU

Department of Mechanical Engineering, İzmir Institute of Technology

Assist.Prof.Dr. H. Seçil ARTEM

Department of Mechanical Engineering, İzmir Institute of Technology

Assist. Prof. Dr. Levent AYDIN

Department of Mechanical Engineering, İzmir Katip Çelebi University

19 December 2013

Prof. Dr. Bülent YARDIMOĞLU

Supervisor, Department of Mechanical Engineering,
İzmir Institute of Technology

Prof. Dr. Metin TANOĞLU

Head of the Department of
Mechanical Engineering

Prof. Dr. R. Tuğrul SENGER

Dean of the Graduate School
of Engineering and Sciences

ACKNOWLEDGEMENTS

This master thesis has been carried out at the Department of Mechanical Engineering, Izmir Institute of Technology, since December 2012. A number of people deserve thanks for their support and help. It is therefore my greatest pleasure to express my gratitude to them all in this acknowledgement.

First of all, I would like to convey my warmest gratitude to my supervisor Professor Dr. Bülent YARDIMOĞLU for his guidance, generous contribution of knowledge and experience, valuable comments and encouragement from the start until the end of my study.

I would also like to thank Barış İSKEÇE, Çetin Özgür BALTACI for their helps and spending time to improve my study.

Furthermore, I would like to acknowledge the help I received from Ercüment ALYANAK, ENA YELKAPAN TEKNOLOJİLERİ. I have benefited from their design parameters.

Finally, I would like to give special thank to my parents and brother for their, helps, patience and supports. Without their support and encouragement, this study would have not been possible.

ABSTRACT

VIBRATION ANALYSIS OF A GIROMILL-TYPE VERTICAL AXIS WIND TURBINE

Vibration characteristics such as natural frequencies and mode shapes of Giromill-type vertical-axis wind turbines (VAWTs) with different design parameters are studied by Finite Element Method (FEM). As design parameters, length of the blade, thickness of the blade and the support distance of the blade are considered. On the other hand, local wind characteristics are considered for aerodynamic calculations.

The well known commercial software package, ANSYS, is used for finite element analysis. Aerodynamic loads and centrifugal forces are taken into account in calculating the natural frequencies.

In order to see the interactions of the parameters of the VAWT, seven models are obtained by modification of model I which is a reference model. Vibration characteristics of all models are found. The obtained results are presented in tabular forms.

ÖZET

DÜŞEY EKSENLİ GIROMILL TİPİ RÜZGAR TÜRBİNİNİN TİTREŞİM ANALİZİ

Giromill tipindeki Düşey Eksenli Rüzgar Türbini (DERT)'nin doğal frekans ve titreşim biçimleri gibi titreşim karakteristikleri, farklı tasarım parametreleri kullanılarak Sonlu Elemanlar Yöntemi (SEY) ile çalışılmıştır. Tasarım parametreleri olarak, kanat uzunluğu, kanat kalınlığı ve kanatın mesnetler arası mesafesi dikkate alınmıştır. Diğer taraftan, aerodinamik hesaplarda bölgesel rüzgar karakteristikleri gözönüne alınmıştır. Sonlu Eleman Analizi için, en bilinen ticari program olan ANSYS kullanılmıştır. Kanat ve diğer türbin elemanları, ANSYS paket programında kiriş elemanlar ile modellenmişlerdir. Doğal frekansların hesaplanmasında aerodinamik yükler ve merkezkaç kuvvetleri dikkate alınmıştır.

DERT'in belirtilen parametreler ile etkileşimini görmek için, referans olan Model I'in değişiklikleri ile yedi model elde edilmiştir. Tüm modellerin titreşim karakteristikleri bulunmuştur. Elde edilen sonuçlar tablolar halinde sunulmuştur.

*Dedicated to my grandfather, Ahmet AKGUNEYLI,
who always pushed me to work hard.*

TABLE OF CONTENTS

LIST OF FIGURES	viii
LIST OF TABLES	ix
LIST OF SYMBOLS	x
CHAPTER 1. GENERAL INTRODUCTION	1
CHAPTER 2. THEORETICAL BACKGROUND	5
2.1. Introduction.....	5
2.2. Geometry of the Giromill-Type VAWT	5
2.3. Geometry of Blade.....	7
2.4. Description of the Problem.....	8
2.5. Aerodynamics of Giromill-Type VAWT	9
2.6. Natural Frequencies and Mode Shapes of the Multi-Degree-of-Freedom Systems.....	12
2.7. Vibration Analysis of Giromill-type VAWT by FEM.....	13
CHAPTER 3. NUMERICAL RESULTS AND DISCUSSION.....	14
3.1. Geometrical Models.....	14
3.2. Finite Element Model of the VAWT	15
3.3. Natural Frequencies and Mode Shapes.....	16
CHAPTER 4. CONCLUSIONS	26
REFERENCES	27

LIST OF FIGURES

<u>Figure</u>	<u>Page</u>
Figure 1.1 Horizontal Axis Wind Turbines (HAWT) and Vertical Axis Wind Turbines (VAWT)	1
Figure 1.2. Savonius type wind turbine	2
Figure 1.3. Darrieus type wind turbine	2
Figure 1.4. A Giromill-type wind turbine	2
Figure 2.1. Giromill-Type VAWT	6
Figure 2.2. Mean line and thickness of the NACA 4 digit wing section	7
Figure 2.3. Upper and lower surface co-ordinates of NACA 4 digit wing section (Source: Abbott 1959)	8
Figure 2.4. Flow velocities of straight-bladed Darrieus-type VAWT (Source: Islam et al 2008)	9
Figure 2.5. Force diagram of a blade airfoil	11
Figure 3.1. Finite element model of VAWT	16
Figure 3.2. First mode shape of Model I	20
Figure 3.3. Second mode shape of Model I	20
Figure 3.4. Third mode shape of Model I	21
Figure 3.5. Fourth mode shape of Model I	21
Figure 3.6. Fifth mode shape of Model I	22
Figure 3.7. Sixth mode shape of Model I	22
Figure 3.8. Seventh mode shape of Model I	23
Figure 3.9. Eighth mode shape of Model I	23
Figure 3.10. Ninth mode shape of Model I	24
Figure 3.11. Tenth mode shape of Model I	24

LIST OF TABLES

<u>Table</u>	<u>Page</u>
Table 3.1. Single parameter modifications for Model I.....	14
Table 3.2. Multiple parameter modifications for Model I.....	14
Table 3.3. Aerodynamic force parameters.....	15
Table 3.4. Single parameter effects for non-rotating system.....	17
Table 3.5. Multiple parameter effects for non-rotating system	17
Table 3.6. Single parameter effects for rotating system	18
Table 3.7. Multiple parameter effects for rotating system.....	18
Table 3.8. Aerodynamic force effects for non-rotating system	19
Table 3.9. Aerodynamic force effects for rotating system	19

LIST OF SYMBOLS

a	induction factor
A	blade support distance shown in Figure 2.1.
B	distance shown in Figure 2.1.
c	chord of the blade
C_d	blade section drag coefficient
C_l	blade section lift coefficient
C_n	blade section normal force coefficient
C_p	power co-efficient
C_t	blade section tangential force coefficient
D	drag force, rotor diameter
$[D]$	damping matrix
E	modulus of elasticity
f_i	i^{th} natural frequencies
$\{f(t)\}$	force vector
F_d	drag force
F_l	lift force
F_n	normal force
F_t	tangential force
$[G]$	geometric stiffness matrix
$[K]$	elastic stiffness matrix
L	length of the blade
m	value of maximum chamber height, lumped mass
N	number of blade
p	position of maximum chamber height
r	leading edge radius
R	radius of H-rotor
Re	Reynold's number
t	maximum thickness of the airfoil
t_w	wall thickness of the blade
$\{u_i\}$	i^{th} vibration mode shape vector
V	velocity of the fluid

V_a	axial flow velocity (induced velocity)
V_c	chordal velocity component
V_n	normal velocity component
V_∞	freestream wind velocity
W	local relative flow velocity
$\{x(t)\}$	displacement vector
(x_u, y_u)	upper surface data points
(x_l, y_l)	lower surface data points
y_c	mean line equation
y_t	thickness distribution
α	angle of attack
γ	blade pitch angle
θ	azimuth angle, angle of mean line gradient
λ	tip speed ratio
μ	dynamic viscosity
ν	poisson ratio, kinematic viscosity of the fluid
ρ	density of the fluid, air and aluminium
σ	solidity
ϕ	connection angle
ω	angular velocity of H-rotor
ω_i	i^{th} natural radian frequency
(\cdot)	differentiation with respect to time

CHAPTER 1

GENERAL INTRODUCTION

A wind turbine is a device that converts wind energy into mechanical energy. Depending on the usage of mechanical energy such as producing electricity or pumping water, the device is called wind turbine or wind pump, respectively. Therefore, the name of the device implies the system characteristics, i.e. windmill and wind charger.

Wind turbines are named considering the rotating axis of the rotor as: Horizontal Axis Wind Turbines (HAWT) and Vertical Axis Wind Turbines (VAWT) which are shown in Figure 1.1. In this section, only VAWT is considered. Aerodynamically, VAWTs can be divided into two groups: (i) Drag based VAWTs: Savonius is shown in Figure 1.2. and (ii) Lift based VAWTs: Darrieus is shown in Figure 1.3.

On the other hand, differently shaped blades are used in VAWT depending on the operating conditions. Troposkien (nearly parabolic) shape blades (see Figure 1.3) or straight blades (see Figure 1.4) are used in the Darrieus type of VAWT. The latter one is known as Giromill-type or H-rotor. Tower structure of the wind turbine is designed either in the tube type or the lattice type.

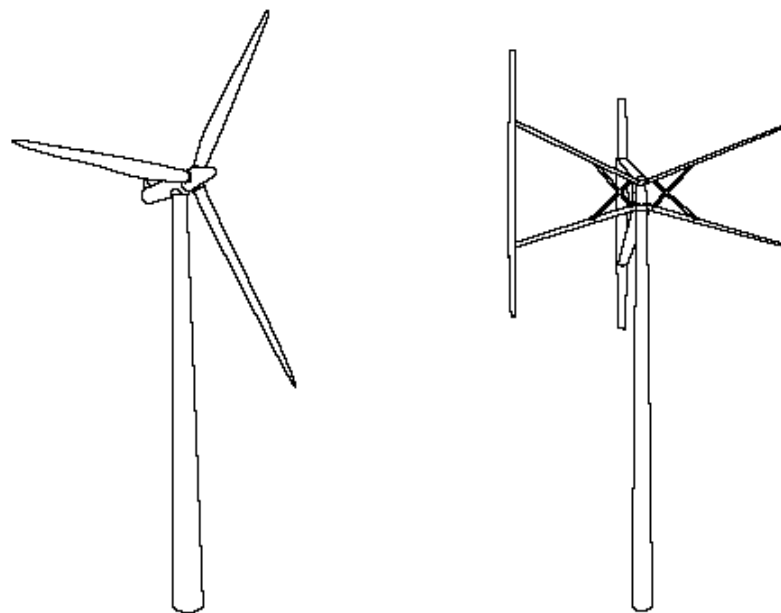


Figure 1.1 Horizontal Axis Wind Turbines (HAWT)
and Vertical Axis Wind Turbines (VAWT)

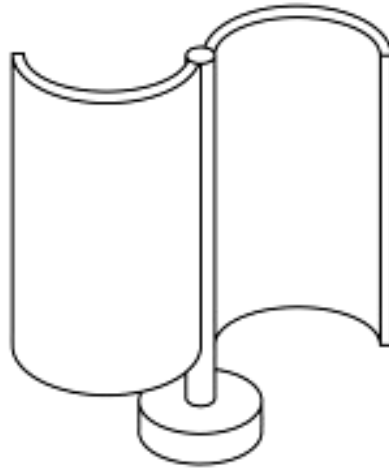


Figure 1.2. Savonius type wind turbine

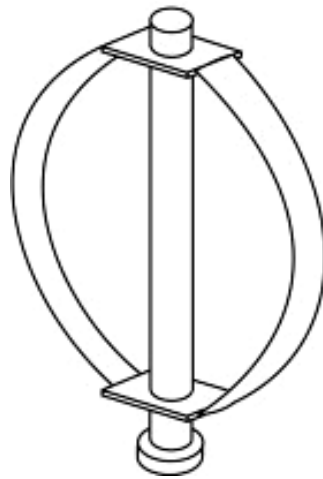


Figure 1.3. Darrieus type wind turbine

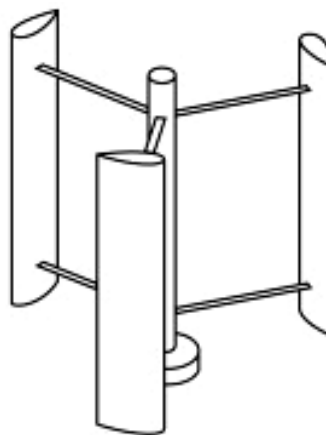


Figure 1.4. A Giromill-type wind turbine

VAWTs have a number of advantages over traditional HAWTs. They are given by Paraschivoiu (2002) as follows:

- Omnidirectional - no yaw equipment.
- Have drive train at ground level: easier to operate and maintain.
- Simpler design - no yaw gear. drop cables, etc.
- Lower cost installation: due to reduced over turning moments and lower tower top mass.
- Have non-cantilevered blade supports.
- May be quieter due to lack of blade tips and ground mounted drive train,
- Unexplored technology may offer more potential for cost reductions.

On the other hand, disadvantages of the VAWTs are listed by Paraschivoiu (2002) as:

- Have a low rotor height which reduces rotor wind speed.
- Have lower tip-speed ratio for peak aerodynamic efficiency. Higher torque means more expensive gearboxes.
- Require more area due to the guy wires.
- Aerodynamic torque ripple provides cyclic loading on drive train.
- Longer blade length, about twice the length of HAWTs. Blades are major wind turbine cost item - low cost blades are essential to VAWTs.

VAWT and HAWT systems have the same general components such as a rotor, a tower, a gearbox, a control system and a foundation. The control system of wind turbine contains an anemometer which continuously measures wind speed.

The range of wind speed can be divided into five groups each of which is characterised by a characteristic wind speed (Hau 2006):

1. Cut-in wind speed: 4-5 m/s
2. Partial-load wind speed
3. Rated wind speed: 15 m/s
4. Full-load wind speed
5. Cut-out wind speed: 25 m/s

The numerical values of wind speeds given above are provided by Paraschivoiu (2002).

Although there are numerous textbooks on wind turbines, the detailed information about the VAWT can be found in limited textbooks on wind turbine written by Paraschivoiu (2002), Spera (2009), Manwell et al (2009), Tong (2010).

Brahimi et al (1995) presented some important findings for aerodynamic models of VAWTs using the streamtube models, the 3-D viscous model, the stochastic wind as well as the numerical simulation of dynamic stall.

Islam et al (2008) attempted to compile the main aerodynamic models that have been used for performance prediction and design of straight-bladed Darrieus-type VAWT.

Paraschivoiu et al (2009) proposed and presented a procedure for computing the optimal variation of the blades' pitch angle of a 7 kW H-Darrieus wind turbine prototype that maximizes its torque at given operational conditions.

Nila et al (2012) reported a brief study on free vibration analysis for determining parameters such as natural frequencies and mode shapes for VAWTs by using available finite element software.

Biadgo et al (2013) investigated the double multiple streamtube (DMST) aerodynamic models on straight blade fixed pitch VAWT having a blade profile designated by NACA0012.

In this study, natural frequencies and mode shapes of rotating Giromill-type VAWTs with different design parameters under centrifugal and aerodynamic loads are studied by FEM. Various length of the blade, thickness of the blade and the support distance of the blade are considered. Local wind characteristics are considered for aerodynamic calculations. In order to see the interactions of the parameters of the VAWT having different design parameters, a series of analysis are performed in ANSYS in which the blade and other member of the VAWTs are modeled by beam elements. The reasonable dimensions of the VAWT are determined for the desired operating conditions.

CHAPTER 2

THEORETICAL BACKGROUND

2.1. Introduction

This chapter is presented to introduce the geometry of the giromill-type VAWT, cross-section of the blade, to describe the problem, aerodynamics of Giromill-type VAWT, to model the system by finite elements and to summarize the vibration analysis of the system.

The detailed information about the VAWT can be found in the special textbook titled as “Wind Turbine Design – With Emphasis on Darrieus Concept” and written by Paraschivoiu (2002). The innovative nature of this book is in its comprehensive review of state of the art in Vertical-Axis Wind Turbine (VAWT). It provides the fundamental concepts to the readers, especially on Savonius and Giromill rotors. It is very useful for the interested readers.

2.2. Geometry of Giromill-Type VAWT

To introduce the parameters of the Giromill-Type VAWT, Figure 2.1 is presented. In this figure, the following parameters are shown:

1. Rotor diameter D
2. Blade length L
3. Blade support distance A
4. Chord length c
5. Ground clearance

Blades of the Giromill-Type VAWT can be modeled as a beam with two overhangs and fixed to upper and lower connecting arms. Moreover, cables are used to provide the stiffness for the frame system.

Number of the blade is chosen as three.

2.3. Geometry of Blade

The NACA 4 digit wing section can be generated by the use of a set of simple polynomial equations. The aerofoils are created by summing a thickness distribution y_t with a given mean line equation y_c which are shown in Figure 2.2.

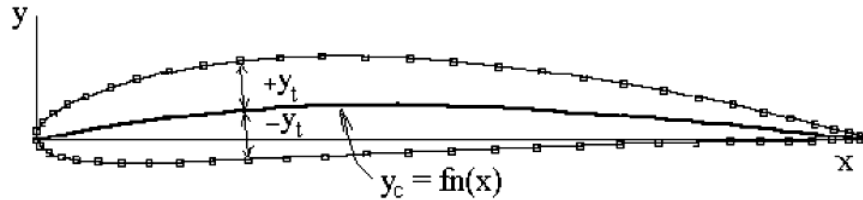


Figure 2.2. Mean line and thickness of the NACA 4 digit wing section

The piecewise function of mean line is given by Abbott (1959) as,

$$y_c = \frac{m}{p^2}(2px - x^2) \quad \text{for } 0 < x < p \quad (2.1)$$

$$y_c = \frac{m}{(1-p)^2}((1-2p) + 2px - x^2) \quad \text{for } p < x < 1$$

where x is a position along the chord line, m is the value of maximum camber height (1/100th chord) and p is the position of maximum camber height (1/10th chord).

The thickness distribution of the aerofoil section y_t is given by Abbott (1959) as,

$$y_t = \frac{t}{0.2}(0.2969\sqrt{x} - 0.126x - 0.3516x^2 + 0.2843x^3 - 0.1015x^4) \quad (2.2)$$

The NACA 4 digit is represented by NACA pmxx. It should be mentioned that NACA 00xx designate a symmetric cross-section since p and m are related with mean line equations. The last two digits xx provide the maximum thickness t of the airfoil in percentage of chord c . For example NACA 0012 means that symmetric section with $t_{\max}=0.12c$.

The construction of the section is then done numerically by identifying surface points which are the sum of camber and thickness effects. Points are normally generated using a cosine distribution of chord x coordinates. For each x coordinate an upper (x_u, y_u) and lower surface (x_l, y_l) data point, shown in Figure 2.3, is generated by applying the following equations:

$$\begin{aligned} x_u &= x - y_t \sin \theta & x_l &= x + y_t \sin \theta \\ y_u &= y_c + y_t \cos \theta & y_l &= y_c - y_t \cos \theta \end{aligned} \quad (2.3)$$

where θ is the angle of the mean line gradient at the coordinate x location.

A leading edge radius r is applied to smooth the front data points and its function is given as

$$r = 1.1019t^2 \quad (2.4)$$

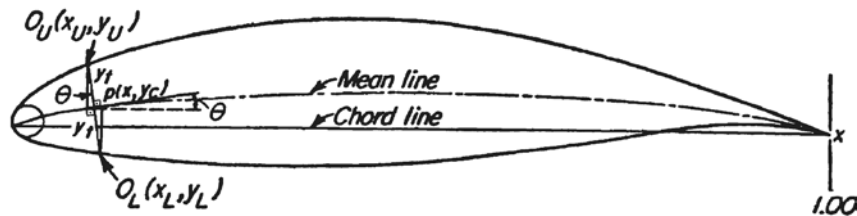


Figure 2.3. Upper and lower surface co-ordinates of NACA 4 digit wing section
(Source: Abbott 1959)

2.4. Description of the Problem

First problem is finding the vibration characteristics such as natural frequencies and mode shapes of rotating Giromill-type VAWTs with different design parameters: type of the aerofoil for the section of the blade, thickness of the blade, chord of the blade, diameter of the rotor, length of the blade. After finding the vibration characteristics of the system under centrifugal and wind loads, the reasonable dimensions of the VAWT are investigated for the desired operating conditions.

2.5. Aerodynamics of Giromill-Type VAWT

In this section, general mathematical expressions for aerodynamic analysis of straight-bladed Darrieus-type VAWTs are presented.

In order to express the variation of local angle of attack α , the velocities shown in Figure 2.4 are considered. The chordal velocity component V_c and the normal velocity component V_n are obtained from the following expressions:

$$V_c = R\omega + V_a \cos \theta \quad (2.5)$$

$$V_n = V_a \sin \theta$$

where V_a is the axial flow velocity (i.e. induced velocity) through the rotor, ω is the rotational velocity, R is the radius of the turbine, and θ is the azimuth angle.

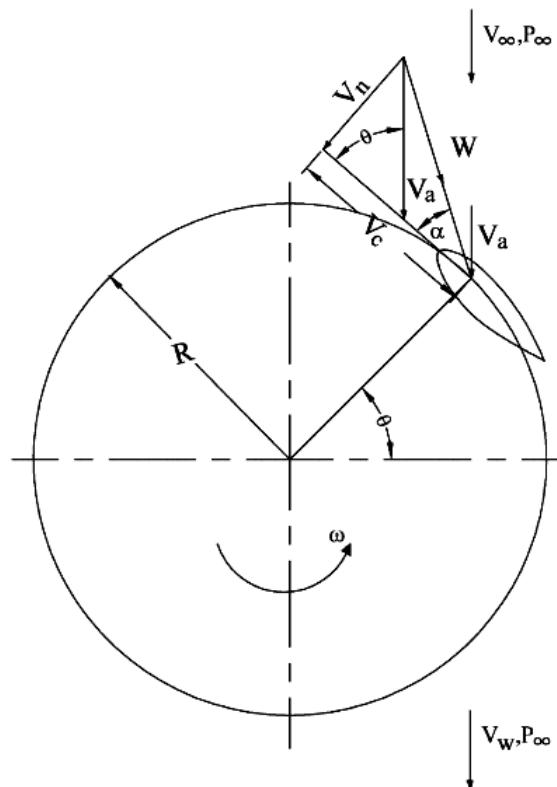


Figure 2.4. Flow velocities of straight-bladed Darrieus-type VAWT

(Source: Islam et al 2008)

The angle of attack α can be expressed as

$$\alpha = \tan^{-1}(V_n / V_c) \quad (2.6)$$

Substituting V_n and V_c into Equation 2.6 and non-dimensionalizing, α can be written as,

$$\alpha = \tan^{-1} \left[\frac{\sin \theta}{(R\omega / V_\infty) / (V_a / V_\infty) + \cos \theta} \right] \quad (2.7)$$

where V_∞ is the freestream wind velocity. If we consider blade pitching then,

$$\alpha = \tan^{-1} \left[\frac{\sin \theta}{(R\omega / V_\infty) / (V_a / V_\infty) + \cos \theta} \right] + \gamma \quad (2.8)$$

where γ is the blade pitch angle. It is clear that local relative flow velocity W is function of the azimuth angle θ . It can be written as

$$W = \sqrt{V_c^2 + V_n^2} \quad (2.9)$$

Substituting the chordal and normal velocity components given by Equation 2.5 into Equation 2.8, and non-dimensionalizing, the following velocity ratio is found

$$\frac{W}{V_\infty} = \frac{W}{V_a} \frac{V_a}{V_\infty} = \frac{V_a}{V_\infty} \sqrt{\left[\left(\frac{R\omega}{V_\infty} / \frac{V_a}{V_\infty} \right) + \cos \theta \right]^2 + \sin^2 \theta} \quad (2.10)$$

The power co-efficient C_p is a function of the tip-speed ratio (TSR) λ for VAWT is given as

$$\lambda = \frac{\omega R}{V_\infty} \quad (2.11)$$

Therefore, Equations 2.7, 2.8 and 2.10 can also be expressed in terms of TSR.

Moreover, it is possible to express a relationship between V_∞ and V_a as

$$\frac{V_a}{V_\infty} = 1 - a \quad (2.12)$$

here a is known as induction factor.

The force diagram of a blade airfoil is shown in Figure 2.5.

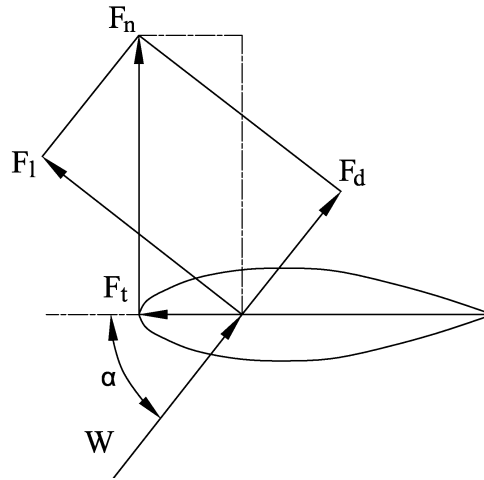


Figure 2.5. Force diagram of a blade airfoil

The net tangential and normal forces are defined as

$$F_t = C_t \frac{1}{2} \rho c L W^2 \quad (2.13)$$

$$F_n = C_n \frac{1}{2} \rho c L W^2 \quad (2.14)$$

where ρ is the air density, c is the blade chord and L is the height of the turbine. The tangential force coefficient C_t and the normal force coefficient C_n used in Equations 2.13 and 2.14 are written as

$$C_t = C_l \sin \alpha - C_d \cos \alpha \quad (2.15)$$

$$C_n = C_l \cos \alpha + C_d \sin \alpha$$

where C_l and C_d are lift and drag force coefficients which are depend on the the angle of attack α and Reynolds number Re . The Reynolds number is expressed as

$$Re = \frac{\rho V c}{\mu} = \frac{V c}{\nu} \quad (2.16)$$

where V is velocity of the fluid, c is the chord width of an airfoil, ρ is the density of the fluid, μ is the dynamic viscosity of the fluid, ν is the kinematic viscosity of the fluid.

Solidity is another important parameter for the VAWT and defined as the ratio of blade area to rotor swept area. It is expressed in open form for N blades as

$$\sigma = \frac{N c}{R} \quad (2.17)$$

2.6. Natural Frequencies and Mode Shapes of the Multi-Degree-of-Freedom Systems

The general differential equation of a forced vibration of the multi-degree-of-freedom system is given by

$$[M]\{\ddot{x}(t)\} + [D]\{\dot{x}(t)\} + ([K] + [G])\{x(t)\} = \{f(t)\} \quad (2.18)$$

where $[M]$, $[D]$, $[K]$ and $[G]$ are mass, damping, elastic stiffness and geometric matrices, respectively. Also, $\{x(t)\}$ is displacement vector and $\{f(t)\}$ is force vector. Considering the harmonic motion for displacement and force vectors in the general differential equation, the following generalized eigenvalue equation is written:

$$([K] + [G] - \omega_i^2 [M])\{u_i\} = \{0\} \quad (2.19)$$

where ω_i is i^{th} natural frequency and $\{u_i\}$ is the i^{th} vibration mode shape vector.

2.7. Vibration Analysis of Giromill-type VAWT by FEM

A Giromill-type VAWT have vertical blades and their radial connecting arms to provide them a rotational motion about vertical axis. Vibration analysis of such a system by distributed-parameter approach is not as simple as by approximate methods. Approximate techniques are used to model the distributed-parameter systems as discrete systems and can be broadly divided into two classes: lumped-parameter methods and series discretization methods. In lumped-parameter methods, the parameters are lumped at discrete points of the system. On the other hand, series discretization methods are based on finite series of trial functions.

The finite element method is very powerful one among the approximate methods due to the available software packages such as ANSYS and ABAQUS. In this study, one dimensional structural element is used to model the system under the rotational and wind loads effects.

CHAPTER 3

NUMERICAL RESULTS AND DISCUSSIONS

3.1. Geometrical Models

In this chapter, numerical analyses are carried out for the Giromill-type vertical-axis wind turbines (VAWTs) with different design parameters. The system and its parameters are shown in Figure 2.1.

The following data are used for all the models: wing type: NACA0015, diameter of the VAWT $D=6$ m, chord of the blade $c=0.3$ m, lumped mass at the connection of blade and connecting arms $m=18$ kg, connection angle $\phi=90^\circ$, angular velocity of the VAWT $\omega=8$ rad/s.

The several models are created by changing a single or multiple parameters of the Model I and given in Table 3.1 and Table 3.2. The modifications are given with bold numbers.

Table 3.1. Single parameter modifications for Model I

Parameters	Model I	Model II	Model III	Model IV
L/R [-]	2	3	2	2
A/L [-]	0.5	0.5	0.67	0.5
t_w [mm]	3	3	3	4

Table 3.2. Multiple parameter modifications for Model I

Parameters	Model V	Model VI	Model VII	Model VIII
L/R [-]	3	3	2	3
A/L [-]	0.67	0.5	0.67	0.67
t_w [mm]	3	4	4	4

3.2. Finite Element Model of the VAWT

The physical models introduced in Section 3.1 are modelled in ANSYS by using BEAM44 elements for blades/connecting arms and MASS21 elements for lumped masses. The finite element model with element numbers is shown in Figure 3.1. Beam elements are numbered from 1 to 20. Lumped mass elements are numbered from 21 to 22. Connecting arms have the same properties with blade properties.

Material properties of the blade and connecting arms are given as follows: Modulus of elasticity $E=70000$ MPa, density of aluminium $\rho=2.73 \cdot 10^{-9}$ ton/mm³ and poisson ratio $\nu=0.3$.

Inner ends of the connecting arms are fixed to the rotor shaft with 600 mm diameter. Instead of modeling the pre-tensioned cable in FEM, corresponding force is acted upon the related node. The value of this force is calculated for approximately zero displacement in the vertical direction for blade in static equilibrium condition.

Geometrical stiffness matrix $[G]$ is based on centrifugal and aerodynamic forces. Pre-stresses due to the centrifugal forces are calculated in ANSYS by static analysis. However, aerodynamic forces are effected to the FEM model using the data given in Table 3.3. Lift and drag coefficients with respect to angle of attack are based on Reynolds numbers. On the other hand, as it is seen from Equation 2.7 along with Equation 2.12, the angle of attack α depends on induction factor a which is assumed as 0.5 (Yardimoglu, 2013). To calculate the Reynolds numbers, average wind speed for Urla/IZMIR is given by Turkish State Meteorological Service as 6 m/s. By using Equation 2.16, Reynolds numbers is found as 126698 for 10°C. Then, lift and drag coefficients are taken from Sheldahl and Klimas (1981) for $Re=160000$.

Table 3.3. Aerodynamic force parameters

θ (°)	α (°)	C_l (-)	C_d (-)	F_n/L (N/mm)	F_t/L (N/mm)
0	0	0	0.0116	0	0.019 in +z direction
90	7	0.715	0.0176	0.0765 in -x direction	0.0075 in +z direction
180	180	0	0.0250	0	0.0015 in +z direction
270	7	0.715	0.0176	0.0765 in +x direction	0.0075 in +z direction

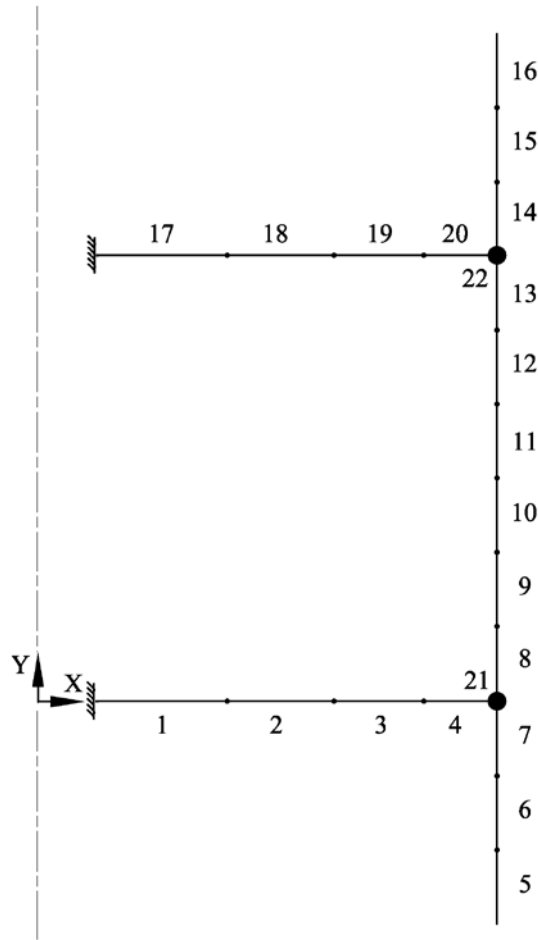


Figure 3.1. Finite element model of VAWT

3.3. Natural Frequencies and Mode Shapes

The natural frequencies of the eight models of present study introduced in Section 3.1 are found by pre-stressed modal analysis that is provided by "pstres,on" in ANSYS. Single parameter effects on Model I detailed in Table 3.1 and multiple parameter effects on Model I detailed in Table 3.2 are investigated in the first step. The results are presented in Tables 3.4 to 3.5 for non-rotating system and in Tables 3.6 to 3.7 for rotating system.

Aerodynamic force effect on the natural frequencies is studied for Model I. The natural frequencies for different azimuth angle θ are given in Tables 3.8 for non-rotating system and in Table 3.9 for rotating system

Finally, the mode shapes for Model I are shown in Figures 3.2.-3.11.

Table 3.4. Single parameter effects for non-rotating system

f_i (Hz)	Model I	Model II	Model III	Model IV
f_1	2.8635	2.4117	2.7580	2.9598
f_2	9.5715	5.3719	8.1534	9.9862
f_3	9.7938	6.4654	10.441	10.308
f_4	11.080	7.6784	14.200	10.821
f_5	13.561	10.322	19.242	13.242
f_6	24.659	10.394	25.720	24.090
f_7	33.584	17.251	26.248	32.941
f_8	34.379	21.255	37.259	33.594
f_9	40.531	30.867	38.379	40.302
f_{10}	65.589	34.255	43.433	64.100

Table 3.5. Multiple parameter effects for non-rotating system

f_i (Hz)	Model V	Model VI	Model VII	Model VIII
f_1	2.3358	2.4632	2.8522	2.3888
f_2	5.2785	5.2855	8.8301	5.1628
f_3	8.6757	6.3317	10.268	8.9870
f_4	9.7307	8.0789	14.137	10.207
f_5	11.479	10.288	19.330	11.216
f_6	13.812	10.355	25.310	13.487
f_7	17.879	17.333	35.746	17.947
f_8	19.641	21.666	37.361	19.188
f_9	31.274	30.180	37.586	30.552
f_{10}	33.878	33.794	42.504	33.182

Table 3.6. Single parameter effects for rotating system

f_i (Hz)	Model I	Model II	Model III	Model IV
f_1	3.1960	2.7812	3.1031	3.2824
f_2	9.6646	5.4655	8.2851	10.074
f_3	9.9027	6.5222	10.620	10.412
f_4	11.238	7.8106	14.277	10.964
f_5	13.655	10.409	19.559	13.328
f_6	24.723	10.418	25.913	24.147
f_7	34.361	17.253	37.117	33.656
f_8	35.063	21.408	37.269	34.220
f_9	40.529	31.547	38.743	40.300
f_{10}	65.766	35.235	43.481	64.261

Table 3.7. Multiple parameter effects for rotating system

f_i (Hz)	Model V	Model VI	Model VII	Model VIII
f_1	2.7354	2.8236	3.1876	2.7809
f_2	5.4547	5.3682	8.9532	5.3364
f_3	8.7876	6.3864	10.436	9.0926
f_4	9.8671	8.2007	14.217	10.340
f_5	11.706	10.370	19.642	11.432
f_6	13.937	10.376	25.519	13.606
f_7	17.921	17.333	36.469	17.990
f_8	19.737	21.827	37.372	19.286
f_9	31.957	30.853	37.967	31.197
f_{10}	34.808	34.650	42.551	34.055

Table 3.8. Aerodynamic force effects for non-rotating system

f_i (Hz)	$\theta=0^\circ$	$\theta=90^\circ$	$\theta=180^\circ$	$\theta=270^\circ$
f_1	2.8635	2.8635	2.8635	2.8940
f_2	9.5715	9.5721	9.5715	9.5797
f_3	9.7938	9.7940	9.7938	9.8031
f_4	11.080	11.081	11.080	11.094
f_5	13.561	13.562	13.561	13.570
f_6	24.659	24.660	24.659	24.665
f_7	33.584	33.585	33.584	33.654
f_8	34.379	34.378	34.379	34.438
f_9	40.531	40.531	40.531	40.530
f_{10}	65.589	65.591	65.589	65.605

Table 3.9. Aerodynamic force effects for rotating system

f_i (Hz)	$\theta=0^\circ$	$\theta=90^\circ$	$\theta=180^\circ$	$\theta=270^\circ$
f_1	3.1960	3.1960	3.1960	3.2233
f_2	9.6646	9.6652	9.6646	9.6727
f_3	9.9027	9.9030	9.9027	9.9120
f_4	11.238	11.239	11.238	11.251
f_5	13.655	13.656	13.655	13.663
f_6	24.723	24.724	24.723	24.728
f_7	34.361	34.363	34.361	34.430
f_8	35.063	35.061	35.063	35.121
f_9	40.529	40.529	40.529	40.529
f_{10}	65.766	65.768	65.766	65.781

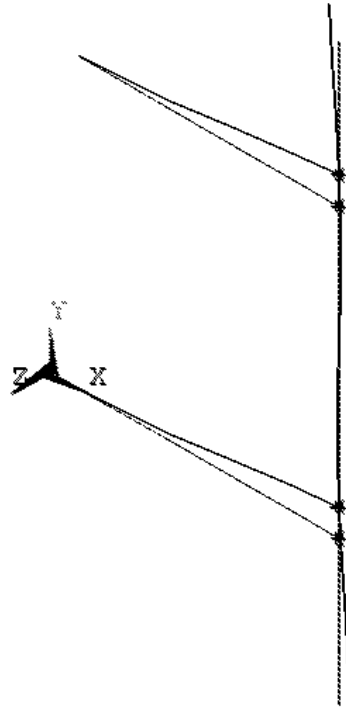


Figure 3.2. First mode shape of Model I

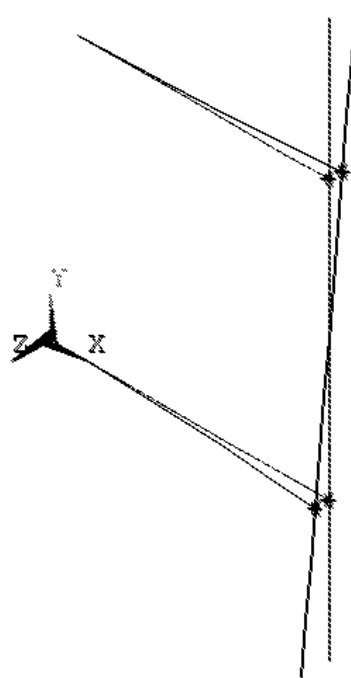


Figure 3.3. Second mode shape of Model I

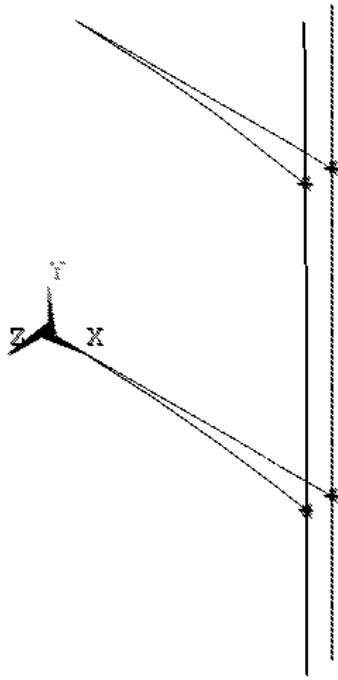


Figure 3.4. Third mode shape of Model I

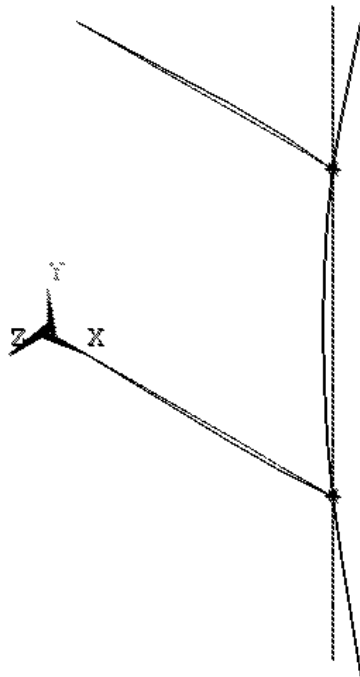


Figure 3.5. Fourth mode shape of Model I

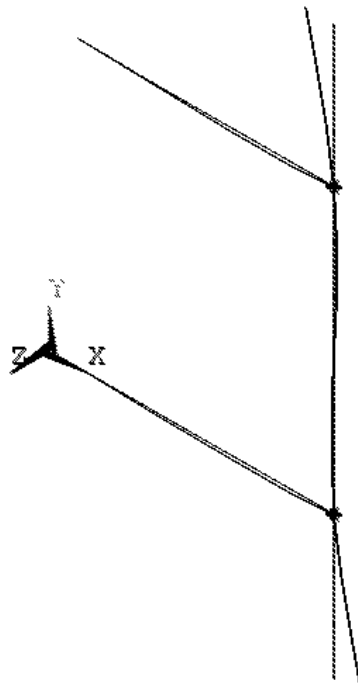


Figure 3.6. Fifth mode shape of Model I

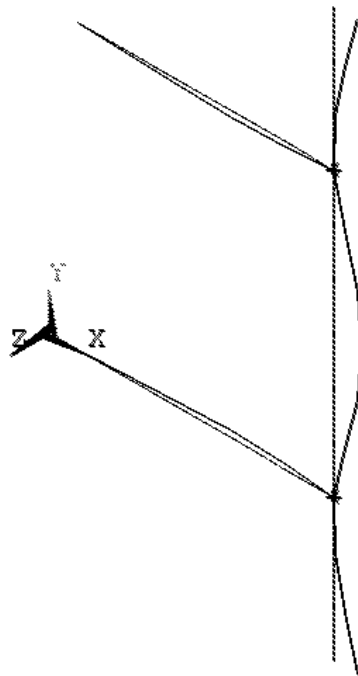


Figure 3.7. Sixth mode shape of Model I

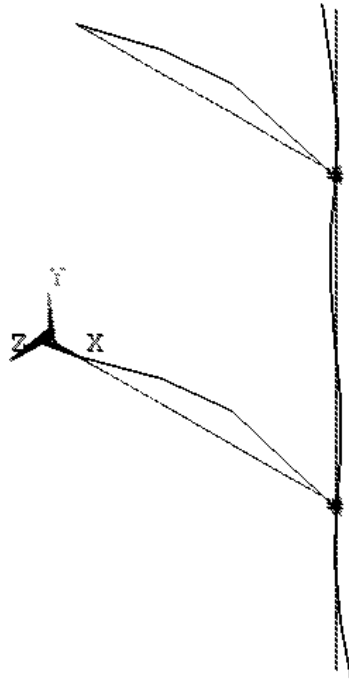


Figure 3.8. Seventh mode shape of Model I

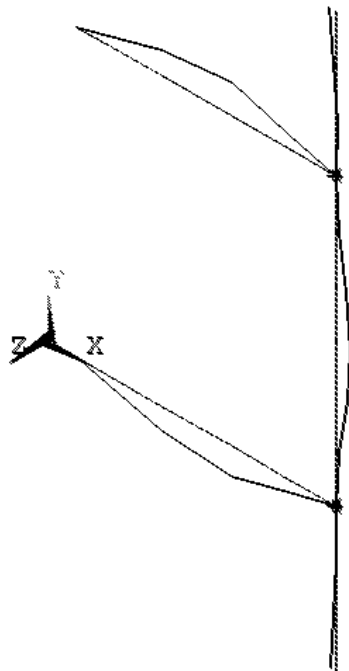


Figure 3.9. Eighth mode shape of Model I

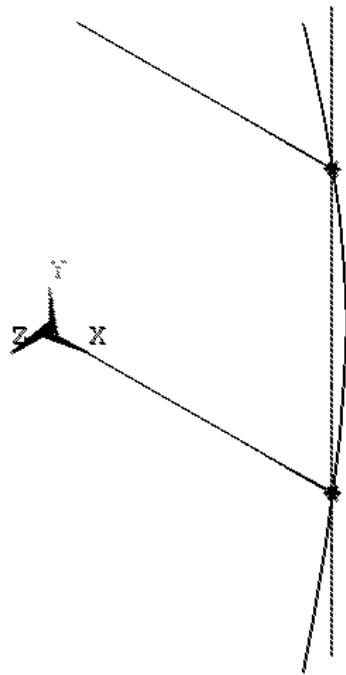


Figure 3.10. Ninth mode shape of Model I

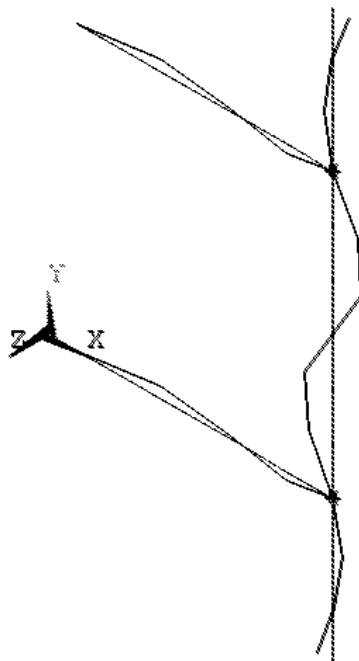


Figure 3.11. Tenth mode shape of Model I

It is very useful to give some important properties about models based on Table 3.1 and 3.2 as follows:

- Model I is reference model.
- Model II has longer blade length L than Model I,
- Model III has longer blade support distance A than Model I,
- Model IV has a greater wall thickness of blade than Model I,
- Model V is combination of Model I and Model III,
- Model VI is combination of Model II and Model IV,
- Model VII is combination of Model III and Model IV,
- Model VIII is combination of Model II, Model III and Model IV.

It is clear from the results of Model I and Model II in Table 3.4 that natural frequencies decrease when blade length L is increased from 6000 mm to 9000 mm.

It is understood from the results of Model I and Model III in Table 3.4 that natural frequencies decrease when blade support distance A is increased from 3000 mm to 4000 mm.

It is found from the results of Model I and Model IV in Table 3.4 that first, second and third natural frequencies increase when the wall thickness of the blade is increased from 3 mm to 4 mm. However, this tendency is reversed for other frequencies.

It can be obtained from Table 3.4 and Table 3.5 that since Model II and Model III with respect to Model I have similar effects on natural frequencies, Model V - which is the combination of the Model II and Model III - has the same tendency for natural frequencies.

Also, it can be found from Table 3.4 and 3.5 that Model VI, Model VII and Model VIII have lower natural frequencies than Model I.

Reviewing the results given in Tables 3.4.-3.7., it is seen that natural frequencies are increased by rotating effects, as expected.

Finally, it is clear from Table 3.4, Table 3.6. Table 3.8 and Table 3.9 that aerodynamic forces are not effective critically on natural frequencies for the present conditions.

CHAPTER 4

CONCLUSIONS

Natural frequencies and mode shapes of giromill-type vertical-axis wind turbines with different design parameters are studied by Finite Element Method (FEM). As design parameters, length of the blade, thickness of the blade and support distance of the blade are considered. The well known commercial software package, ANSYS, is used for finite element analysis. Aerodynamic loads and centrifugal forces are taken into account in calculating the natural frequencies.

In order to see the interactions of the parameters of the VAWT, a series of analysis are performed. The obtained results are presented in tabular forms. It is seen that aerodynamic forces in the present operating condition is not critical for natural frequencies. However, centrifugal force is effective on natural frequencies.

REFERENCES

- Abbott, I.H. 1959, Theory of wing sections. New York: Dover Publications.
- Auld, D.J. and Srinivas, K. 2013, Aerodynamics for students, web textbook, <https://sites.google.com/site/aerodynamics4students/>
- Biadgo, A.M., Simonovic, A., Komarov, D. and Stupar, S. 2013 Numerical and Analytical Investigation of Vertical Axis Wind Turbine *Faculty of Mechanical Engineering, Belgrade* ,41: 49-58.
- Brahimi, M.T., Allet, A and Paraschivoiu, I. 1995. Aerodynamic Analysis Models for Vertical-Axis Wind Turbines *International Journal of Rotating Machinery* , 2, 15-21.
- Hau, Eric 2006. Wind Turbines. Berlin: Springer
- Islam, M., Ting, D.S.K. and Fartaj, A. 2008. Aerodynamic models for Darrieus-type straight-bladed vertical axis wind turbines. *Renewable and Sustainable Energy Reviews*, 12: 1087–1109.
- Love, A. E. H. 1944. A treatise on the mathematical theory of elasticity. New York: Dover Publications.
- Meirovitch, Leonard 1967. Analytical methods in vibrations. New York: Macmillan Publishing.
- Nila, I., Bogateanu, R., Stere, M. and Baran, D. 2012 Modal analysis of a small vertical axis wind turbine (Type Darrieus) *INCAS BULLETIN*, 4, 75 – 81.
- Paraschivoiu, Ion 2002. Wind turbine design: Canada: Polytechnic International Press
- Paraschivoiu, I., Trifu, O. and Saeed, F. 2009. H-Darrieus Wind Turbine with Blade Pitch Control *International Journal of Rotating Machinery*, Vol. 2009, Article ID 505343, 7 pages. (2009)

Popov, E. P. and Balan, T. A. 1998. Engineering Mechanics of Solids. New Jersey: Prentice Hall.

Sheldahl, R. E. and Klimas, P. C. 1981. Aerodynamic characteristics of seven symmetrical airfoil sections through 180-degree angle of attack for use in aerodynamic analysis of vertical axis wind turbines. Report SAND80-2114, Sandia Laboratories, Albuquerque.

Yardimoglu, Bulent 2013. Lecture Notes on Vibrations of Wind Turbines, Izmir: Izmir Institute of Technology.